JOURNAL OF VIROLOGY, June 2003, p. 6245–6254 Vol. 77, No. 11
0022-538X/03/$08.00+0 DOI: 10.1128/JVI.77.11.6245–6254.2003

Resolution of Parvovirus Dimer Junctions Proceeds through a Novel Heterocruciform Intermediate

Susan F. Cotmore[1] and Peter Tattersall[1,2]*

Departments of Laboratory Medicine[1] and Genetics,[2] Yale University School of Medicine, New Haven, Connecticut 06510

Received 9 December 2002/Accepted 12 March 2003

The minute virus of mice initiator protein, NS1, excises new copies of the left viral telomere in a single sequence orientation, dubbed flip, during resolution of the junction between monomer genomes in palindromic dimer intermediate duplexes. We examined this reaction in vitro using both ^{32}P-end-labeled linear substrates and similar unlabeled templates labeled by incorporation of [α-^{32}P]TTP during the synthesis. The observed products suggest a resolution model that explains conservation of the hairpin sequence and in which a novel heterocruciform intermediate plays a crucial role. In vitro, NS1 initiates two replication pathways from OriL$_{TC}$, the single active origin embedded in one arm of the dimer junction. NS1-mediated nicking liberates a base-paired 3′ nucleotide to prime DNA synthesis and, in a reaction we call "read-through synthesis," forks established while the substrate is a linear duplex synthesize DNA in the flop orientation, leading to DNA amplification but not to junction resolution. Nicking leaves NS1 covalently attached to the 5′ end of the DNA, where it can serve as a 3′-to-5′ helicase, unwinding the NS1-associated strand. In the second pathway, resolution substrates are created when such unwinding induces the palindrome to reconfigure into a cruciform prior to fork assembly. New forks can then synthesize DNA in the flip orientation, copying one cruciform arm and creating a heterocruciform intermediate. Resolution proceeds via hairpin transfer in the extended arm of the heterocruciform, which releases one covalently closed duplex telomere and a partially single-stranded junction intermediate. We suggest that the latter intermediate is finally resolved via an NS1-induced single-strand nick at the otherwise inactive origin, OriL$_{GAA}$.

The parvovirus minute virus of mice (MVM) has a negative-sense linear DNA genome in which a single-stranded coding region (of 4,805 nucleotides) is bracketed between imperfect terminal palindromes of 121 and 246 nucleotides at the left (3′) and right (5′) ends, respectively (14). These telomeres play a critical role in rolling hairpin replication, the modified rolling circle replication (RCR) mechanism adopted by MVM, both by providing the sequence elements that serve as viral replication origins and by operating as "toggle switches," alternately folding back on themselves and then unfolding, to adapt the RCR strategy for the replication of a linear chromosome.

MVM DNA is amplified through a series of monomeric and concatemeric duplex replicative-form (RF) intermediates by a unidirectional, leading-strand-specific, cellular replication fork, aided and orchestrated by a single multifunctional viral initiator protein, NS1 (13, 18). Like other RCR initiators, NS1 is a site-specific duplex DNA binding protein with site-specific, single-strand nickase activity. It activates replication by binding to its duplex recognition sequence, $(ACCA)_n$, present in all viral origins, and introducing a strand-specific, single-strand nick at an adjacent initiation site. This transesterification reaction creates a base-paired 3′ nucleotide to serve as a primer for new DNA synthesis while leaving NS1 covalently attached to the 5′ end of the DNA at the nick site, where it likely serves as a 3′-to-5′ helicase (9). The available evidence suggests that NS1 may also operate the toggle-switch mechanisms which unfold and refold the viral hairpins (22, 23), although these reactions remain to be elucidated in detail.

The initial rolling hairpin model (21) predicted that any terminus which was not a perfect palindrome would be produced with equal frequency in two sequence orientations, called flip and flop, which are the inverted complements of one another. While this prediction holds for the MVM right-end hairpin, the left (viral 3′) end of the genome is present in both packaged virus and intracellular viral RF DNA in only a single orientation, dubbed flip, as shown in Fig. 1 (1, 2). Moreover, while the right end of the genome serves as an NS1-dependent origin in its hairpin configuration (3, 15), the origin associated with the left end is silent until the hairpin is extended and copied during replication to form the fully base-paired, dimer bridge region, which spans adjacent genomes in dimer RF (10, 17).

Figure 1 details how the sequence of the 3′ hairpin is unfolded and copied in this dimer junction sequence, with particular reference to internal palindromic sequences, designated the "ears," and an asymmetric mismatched "bubble" within the stem of the hairpin. In the flip orientation of the hairpin, this bubble contains the triplet 5′-GAA on the inboard strand of the hairpin stem, aligned with the doublet 5′-GA on the outboard strand. In the bridge arrangement, these nucleotides are base-paired to their complementary sequences, TTC and TC, respectively. OriL$_{TC}$, the minimal left origin of MVM is a fully duplex, 50-bp sequence derived from the B arm of the bridge as depicted in Fig. 1, which contains the dinucleotide bubble sequence. The equivalent sequence, oriL$_{GAA}$, from the inboard A arm, which is identical except for the bubble trinucleotide, is inactive. We have previously shown that it is predom-

* Corresponding author. Mailing address: Department of Laboratory Medicine, Yale University School of Medicine, 333 Cedar St., New Haven, CT 06510. Phone: (203) 785-4586. Fax: (203) 688-7340. E-mail: peter.tattersall@yale.edu.

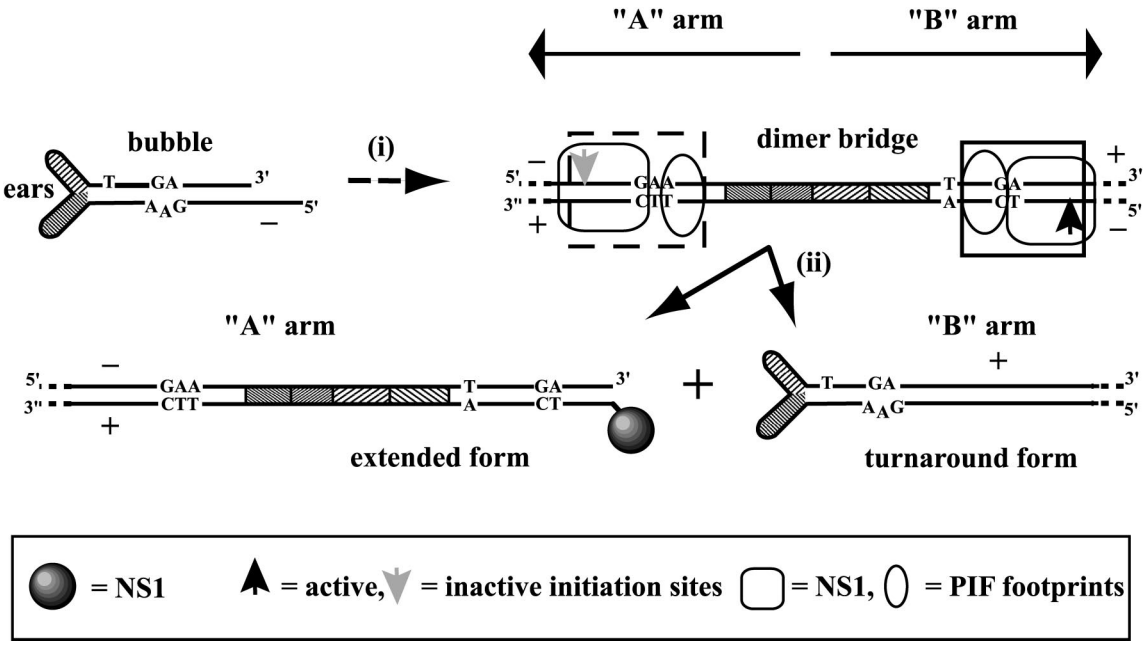

FIG. 1. Structure of the MVM dimer bridge. Step i shows how the left-end hairpin, in its normal flip orientation, is unfolded and copied to create the duplex, palindromic junction that spans adjacent genomes in dimer RF. Negative- and positive-sense strands with respect to transcription are denoted by the symbols − and +. Cross-hatched boxes represent internal palindromic sequences that fold to create the ears in the hairpin form. Mismatched nucleotides in the stem are shown, with the bubble sequence referring to the asymmetry which controls the distribution of the active and inactive origins in the bridge arrangement. Step ii indicates the major products of an in vitro resolution reaction using supercoiled plasmid templates containing the junction sequence (10).

inantly the number, and not the sequence, of nucleotides in this bubble element which regulates initiation (12) and that it acts by modifying the distance between the NS1 binding site and the binding site for an essential cellular cofactor, called parvovirus initiation factor, or PIF (7, 8).

PIF and NS1 bind site specifically to both oriL_{TC} and oriL_{GAA}, but these interactions are only cooperative on oriL_{TC}, forming a ternary complex that effectively stabilizes the interaction of NS1 with OriL_{TC} during ATP hydrolysis (6). Like other RCR initiators, NS1 can only nick single-stranded forms of its initiation site (19). Nicking at duplex oriL_{TC} thus requires ATP hydrolysis to fuel the unwinding activity that melts the duplex substrate and presents the nick site to the nickase as single-stranded DNA. Without this cooperative interaction between NS1 and PIF, the duplex nick site remains silent, as in oriL_{GAA}. This distinction between the ability of NS1 to nick single-stranded forms of its nick site unaided by cofactors and the strict requirement for cofactors to allow nicking at duplex forms is an important aspect of the resolution model presented here.

This tight control means that NS1 is only able to introduce one single-stranded nick into the duplex bridge sequence, into the active initiation site in the lower strand of the B arm, as shown in Fig. 1. A new fork initiated at this site on a linear substrate would synthesize DNA in the flop orientation, ultimately recreating the linear duplex and displacing one positive-sense single strand. We observed this type of reaction in the experiments described here and designate it "read-through synthesis." We suggest that it represents an amplification, rather than a full resolution, pathway and that such products are not the only outcome of initiation at OriL_{TC}.

We have previously shown that templates containing the dimer bridge sequence as part of a supercoiled plasmid can be resolved in vitro using cellular replication extracts and recombinant NS1 to generate two new duplex viral termini, one associated with each arm of the junction palindrome. This resolution was found to be somewhat asymmetric, as shown in Fig. 1, generating predominantly NS1-associated "extended forms" of the A arm, while the B arm was most frequently represented as "turn-around" hairpin forms in which the two strands of the duplex were covalently continuous through the axis of symmetry (10, 17).

Here we reexamine the dimer resolution reaction in vitro, using linear substrates and develop a resolution model based on the structure and temporal expression of three resolution intermediates, which we call MJ1, MJ2, and δJ, and on the distribution of newly synthesized DNA. Evidence is presented that supports the characterization of MJ2 as a heterocruciform structure. The proposed mechanism relies on characteristic parvoviral duplex-to-hairpin rearrangements of the palindrome, mediated by NS1, to explain bridge resolution and the generation of negative-sense genomes with left-end telomeres exclusively in the flip orientation.

MATERIALS AND METHODS

Templates. The pUC18-based plasmid pLEB711, containing a palindromic, 711-bp *Pst*I fragment (MVM nucleotide 415) derived from the left end to the left-end junction of dimeric RF DNA, has been described previously (16). A 2,103-bp *Ase*I fragment containing the dimer bridge was excised, and the ends were filled with unlabeled TTP and dATP by using Sequenase (U.S. Biochemical, Cleveland, Ohio) or they were 3′ end labeled with [α-^{32}P]TTP and unlabeled dATP.

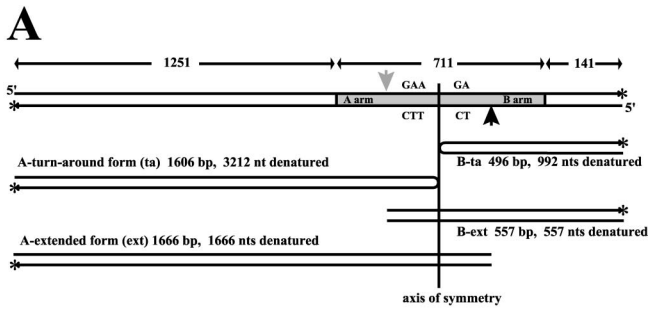

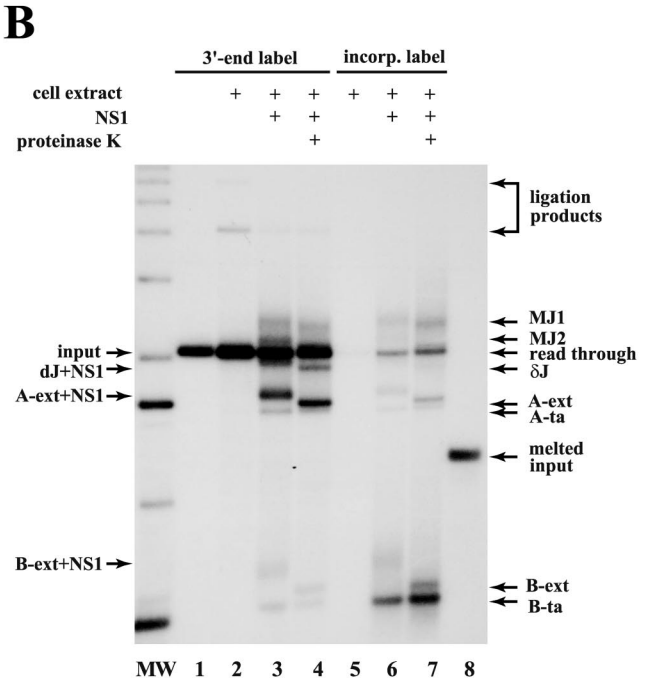

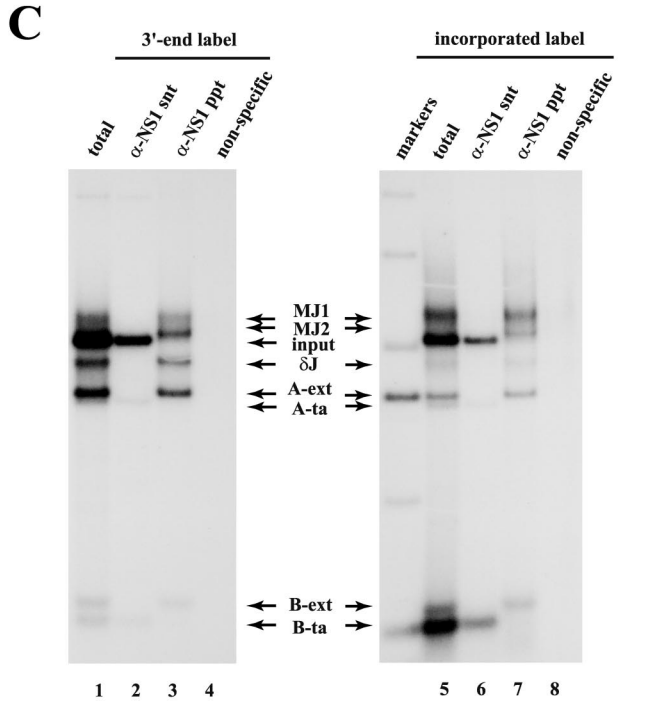

Resolution assays. Recombinant histidine-tagged MVM NS1 was expressed in HeLa cells from recombinant vaccinia virus and purified by nickel-chelate chromatography as previously described (20). Recombinant RPA, expressed from baculovirus vectors and purified as described elsewhere (9), was kindly provided by Jesper Christensen. Replication extracts were prepared from uninfected A9 cells essentially as described by Wobbe et al. (24), except that they were dialyzed against 20 mM Tris-HCl (pH 7.5), 0.2 mM EDTA, 25 mM NaCl, 0.5 mM dithiothreitol, 10% glycerol, and 10% sucrose, which concentrated the extracts approximately twofold. Assays were carried out as previously described (11), in a volume of 20 μl that contained recombinant NS1 (2.5 μg/ml), deoxynucleotides, $MgCl_2$, ribonucleotides, ATP, and an ATP-regenerating system, and either ^{32}P-3′-end-labeled template DNA (1.25 μg/ml) or unlabeled, blunt-ended template DNA plus [α-^{32}P]TTP. Reactions were terminated by addition of sodium dodecyl sulfate (SDS) and EDTA to final concentrations of 0.5% and 5 mM, respectively, and analyzed on neutral agarose gels (one dimension) or neutral followed by alkaline agarose gels (two dimensions), as described previously (11). Samples to be immunoprecipitated were incubated in buffer containing 2% SDS at 60°C for 20 min to disrupt noncovalent interactions, diluted, and precipitated with rabbit antiserum directed against the N-terminal domain of NS1. Unless otherwise specified, neutral agarose gels contained 0.2% SDS in both gel and buffer.

RESULTS

Resolution products of linear dimer bridge substrates. Linear substrates containing a 711-bp cloned copy of the MVM dimer bridge positioned asymmetrically in vector sequences are shown in Fig. 2A. Use of an asymmetric substrate allowed us to distinguish resolution products of around 1.6 kb derived from the A arm of the bridge from those of around 0.5 kb derived from the B arm. To identify the synthetic steps asso-

FIG. 2. Resolution products of ^{32}P-3′-end-labeled linear templates and of similar unlabeled templates, labeled by incorporation of [α-^{32}P]TTP into newly synthesized DNA. (A) Diagram of the 2,103-bp linear *Ase*I template containing an asymmetrically placed 711-bp MVM dimer bridge sequence (grey box). The axis of symmetry separates the A arm of the bridge, containing the inactive duplex origin sequence $OriL_{GAA}$, from the B arm of the bridge containing the active origin, $OriL_{TC}$. The active and inactive NS1 nick sites in these sequences are marked by a dark and light arrow, respectively. Asterisks mark the position of ^{32}P label present in 3′-end-labeled substrates. The predicted sizes of extended and turn-around forms of each arm are specified. (B) Autoradiograph of a 1.4% neutral agarose gel containing 0.2% SDS. ^{32}P-3′-labeled substrates are shown before (0.5× concentration, lane 1) and after (lane 2) incubation with cell extract alone or cell extract supplemented with recombinant NS1 (lanes 3 and 4). Unlabeled substrates incubated with [α-^{32}P]TTP in the presence of cell extract alone are shown in lane 5, and those with extract supplemented with NS1 are shown in lanes 6 and 7. Samples in lanes 4 and 7 were digested with proteinase K prior to electrophoresis. The single-stranded form of the ^{32}P-3′-labeled substrate, melted by incubation at 95°C for 5 min, is shown in lane 8. "A ext" and "B ext" denote extended forms of the A and B arms of the template (as depicted in panel A), while "A ta" and "B ta" denote turn-around forms. MJ1 and MJ2, for modified junction fragments 1 and 2, and δJ denote putative resolution intermediates. Fragments denoted "+NS1" are still covalently associated with NS1 and so show retarded migration relative to their proteinase-treated neighbors. (C) Autoradiograph of a 1.4% neutral agarose gel containing 0.2% SDS. The resolution products of ^{32}P-3′-labeled templates are shown in lanes 1 to 4, and the products labeled by incorporation of [α-^{32}P]TTP into newly synthesized DNA are shown in lanes 5 to 8, before (lanes 1 and 5) and after (lanes 4 and 8) immunoprecipitation with nonspecific rabbit serum or anti-NS1-specific serum (lanes 3 and 7). Unbound materials from the anti-NS1 precipitates are shown in lanes 2 and 6. All samples were digested with proteinase K prior to electrophoresis. Fragments are labeled as detailed for panel B.

ciated with resolution, we compared the products of ^{32}P-3′-end-labeled linear templates, where we could monitor the fate of each input strand, with products generated from similar, but unlabeled, substrates which were labeled during the course of the reaction by incorporation of [α-^{32}P]TTP into newly synthesized DNA.

(i) Resolution products of 3′-end-labeled linear substrates. When incubated with A9 cell extracts in the absence of NS1, ^{32}P-3′-end-labeled linear fragments containing the dimer bridge showed little evidence of modification (Fig. 2B, compare lanes 1 and 2), although some dimeric and trimeric ligation products were generated. Such ligation products are the inevitable consequence of incubating blunt-ended substrates in cell extracts, but they are likely irrelevant for MVM replication in vivo, since viral replication intermediates do not have exposed blunt ends. In contrast, when NS1 was included in the reaction mixture (lane 3), much of the input DNA was modified, generating the expected duplex resolution products (extended and turn-around forms of the A and B arms), together with three higher-molecular-weight species (labeled MJ1 and MJ2, for modified junction 1 and 2, and δJ) which are potential resolution intermediates. In the following analyses we show, in detail, the structure of each of these products and intermediates.

As observed previously using supercoiled dimer bridge substrates labeled by [α-^{32}P]TTP incorporation (10), resolution of the linear substrates appeared asymmetric, in that extended forms of the A arm greatly outnumbered its turn-around form. However, in the present analysis, extended and turn-around forms of the B arm often appeared approximately equimolar and were greatly outnumbered by duplex forms of the A arm.

The native agarose gel shown in Fig. 2B contained SDS, allowing fragments that were covalently associated with NS1 to enter the gel. When a sample equivalent to the one shown in lane 3 was digested with proteinase K prior to electrophoresis (lane 4), potential intermediates MJ1, MJ2, δJ, and extended forms of the A and B arms showed enhanced mobility, indicating that they were initially covalently complexed with NS1. In contrast, unit-length input molecules and turn-around forms of the A and B arms were not NS1 associated and remained in the unbound fraction following immunoprecipitation (Fig. 2C, lane 2).

Since MJ1 and MJ2 forms migrated more slowly than input DNA even after proteinase K digestion, they likely contained more DNA than the input, while δJ migrated faster than input, suggesting that it had lost DNA. None of the observed forms comigrated with denatured template (Fig. 2B, lane 8), confirming that they were not simply melted-out forms of the substrate.

(ii) Products labeled by incorporating [α-^{32}P]TTP into newly synthesized DNA. In the absence of NS1, unlabeled linear fragments containing the dimer bridge were barely labeled in vitro (Fig. 2B, lane 5). Introducing NS1 into the reaction mixture (lane 6) resulted in the appearance of newly synthesized DNA in a variety of species, including unit-length linear molecules that comigrated with the 3′-end-labeled input DNA shown in lane 1. Digestion with proteinase K did not affect the mobility of this product (lane 7), and it did not immunoprecipitate with anti-NS1 serum (Fig. 2C, compare lanes 6 and 7), indicating that it was not covalently associated with NS1 even though NS1 was required for its synthesis (Fig. 2B, compare lane 5 with lanes 6 and 7). We suggest that these labeled unit-length molecules are the products of read-through replication (discussed below), which allows DNA amplification without junction resolution.

Surprisingly, the resolution product which contained most of the newly synthesized DNA was the turn-around form of the B arm. This product was identified as a B turn-around form because it migrated at ~0.5 kb under neutral conditions but migrated at ~1 kb under denaturing conditions (see below), indicating that the strands of the duplex were covalently continuous at one end. In addition, this DNA species was not directly associated with NS1, as confirmed by its presence in the unbound fraction of the anti-NS1 immunoprecipitate shown in Fig. 2C, lane 6.

All fully resolved forms of the bridge (i.e., extended and turn-around forms of both the A and B arms) contained at least some newly synthesized DNA, as did the NS1-associated MJ1 and MJ2 intermediates (Fig. 2C, lane 7). In contrast, the δJ intermediate was not significantly labeled by in vitro synthesis (compare Fig. 2B, lane 4 with 7, and 2C, lane 3 with 7), suggesting that it did not contain significant stretches of newly synthesized DNA.

Read-through synthesis. Unit-length duplex molecules labeled by incorporation of [α-^{32}P]TTP into newly synthesized DNA in the NS1-dependent reaction (Fig. 2B, lanes 6 and 7, and C, lanes 5 and 6) are products of a type of reaction we call read-through synthesis, which does not lead directly to the generation of duplex resolution products. In the amplification pathway depicted in Fig. 3A, a leading-strand-specific cellular fork, which can be assembled in vitro with recombinant RPA, RFC, PCNA, and DNA polymerase δ (S. F. Cotmore, J. Christensen, and P. Tattersall, unpublished results), forms rapidly on the newly available 3′ hydroxyl (step i), allowing strand displacement synthesis to occur on the linear template (step ii). This displaces an NS1-associated, single-stranded, positive-sense form of the A arm, while replacing it with labeled, newly synthesized DNA (step iii). Displaced single-stranded forms of the A arm were identified in the resolution products of 3′-end-labeled substrates, but they migrated as a diffuse band in the SDS-agarose gels shown here and were minor products, perhaps because single-stranded DNA is more susceptible to degradation than duplex DNA in complex cell extracts. In Fig. 3B, lane 1, we show proteinase K-digested products of an NS1-driven reaction displayed on a non-SDS gel. Single-stranded forms of the A arm can be identified in these products, but they become particularly apparent when compared to products shown in lane 2, where the release of single-stranded forms has been promoted by the inclusion of a large molar excess of recombinant RPA. Their identity as NS1-associated 1.6-kb single strands was confirmed by two-dimensional gel electrophoresis and by their specific immunoprecipitation with anti-NS1 serum (data not shown).

Since the dimer bridge remains in the linear configuration throughout this read-through reaction, new DNA would be synthesized in the flop orientation on the negative-sense primer strand (Fig. 3A, step ii). However, since this reaction does not appear to lead directly to resolution of the resulting duplex product, no termini in the flop orientation would be excised.

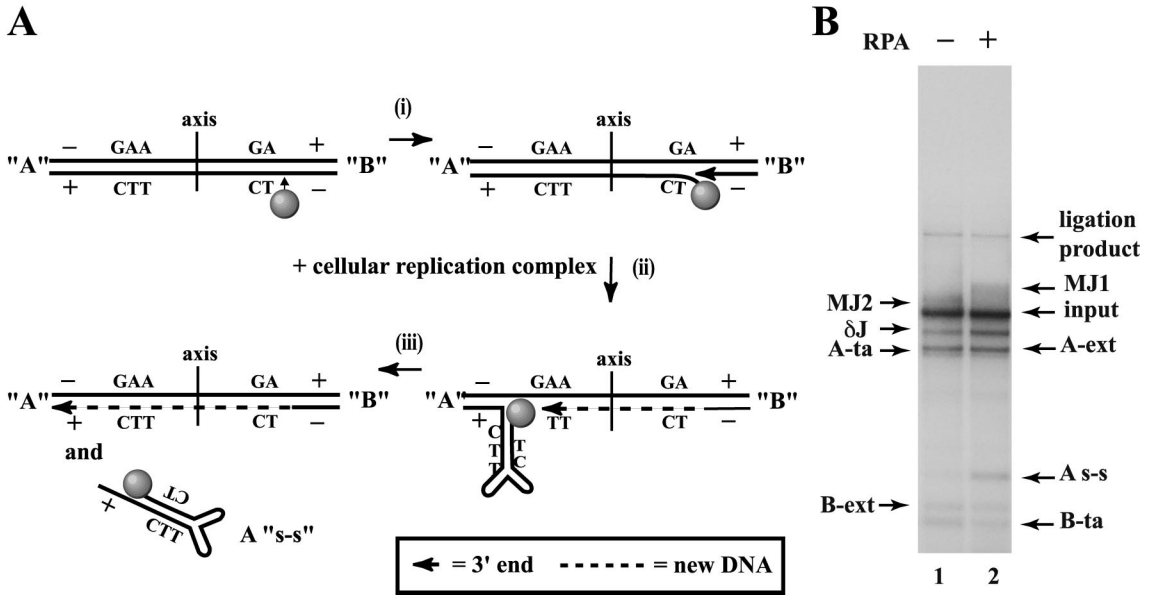

FIG. 3. Read-through synthesis. (A) Diagram of read-through synthesis, as discussed in the text. "A s-s" denotes the single-stranded form of the A arm, with its 5′ hairpin; "axis" is the symmetry axis of the junction; other symbols are as detailed in the legend for Fig. 1. (B) Autoradiograph of a 1.4% neutral agarose gel (without SDS) showing resolution products of ^{32}P-3′-end-labeled templates incubated in a standard, NS1-supplemented, resolution mix (lane 1) or in a mix supplemented with recombinant RPA (25 μg/ml). Fragments are labeled as detailed for Fig. 2B.

Time course of the resolution reaction. Products generated and labeled by incorporation of [α-^{32}P]TTP into newly synthesized DNA were analyzed, at intervals during the course of a 2-h reaction, by electrophoresis through neutral SDS-agarose gels, both before (Fig. 4A, lanes 2 to 8) and after (Fig. 4A, lanes 9 to 12) proteinase K digestion. During the first 90 min of the reaction, the rate of [α-^{32}P]TTP incorporation into DNA was approximately linear, but declined thereafter. The clear redistribution of incorporated label with time, from higher-molecular-weight structures at the earliest time points to the final resolution products after 1 to 2 h, suggests that this reaction was relatively synchronous and that initiation was most common early during synthesis, perhaps because active NS1 concentrations became limiting thereafter.

The major labeled species observed in samples incubated for 30 min or less (Fig. 4A, lanes 2 to 5) were the MJ intermediates and unit-length linear molecules, presumably labeled by read-through synthesis as discussed above. Notably, while the MJ2 form appeared early, its concentration remained fairly constant with time, while the more heterogeneous MJ1 forms increased in concentration during the first 30 min but declined significantly thereafter, as extended and turn-around forms of both arms, but most notably turn-around forms of the B arm, accumulated. This suggests that MJ1, in particular, is an active intermediate in the generation of new termini.

Generation and processing of ^{32}P-3′-end-labeled substrates were also analyzed as a function of time in an NS1-dependent reaction (Fig. 4B). Analysis of total reaction products harvested at 30-min intervals (lanes 1 to 3) and species immunoprecipitated from reactions with anti-NS1 serum (lanes 4 to 6) showed that the heterogeneous MJ1 species appeared early and declined with time, while the δJ intermediate progressively accumulated. Residual input DNA remained in the unbound fraction of these precipitates (lanes 7 to 9), together with turn-around forms of the resolution products.

Structures of MJ1, MJ2, and δJ intermediates. Products generated and labeled by incorporation of [α-^{32}P]TTP into newly synthesized DNA from the 60-min time point were digested with proteinase K (as in Fig. 4A, lane 10) and further analyzed by two-dimensional electrophoresis under native and then denaturing conditions (Fig. 5A). This type of analysis allowed us to distinguish extended forms of the telomeres, where the two strands of the duplex were free to separate under denaturing conditions, from turn-around forms, where the two strands were held together covalently at one end. Thus, extended forms of the B arm migrated as ~0.5-kb duplexes in the first dimension and as ~0.5-kb single strands in the second, while turn-around forms of the B arm migrated as somewhat smaller duplexes than extended forms but appeared almost twice as long (approximately 1 kb) when denatured.

These gels also allowed us to dissect high-molecular-weight products and intermediates and thus to identify what types of DNA fragment contained newly synthesized DNA. Unit-length linear molecules, presumably labeled by read-through synthesis, migrated as labeled ~2-kb duplexes in the first dimension and as ~2-kb single strands in the second, indicating that the new DNA was contained within full-length DNA strands. In contrast, none of the new DNA in the MJ1 and MJ2 intermediates was associated with a full-length strand. Instead, most of the new DNA in the MJ2 intermediate was present in a single strand of approximately 0.5 kb which comigrated in the alkaline dimension with extended forms of the B arm. In Fig. 5D we suggest a heterocruciform structure for this MJ2 intermediate, in which new DNA is confined to an extended form of the B arm. This newly synthesized DNA is predicted to be in the flip orientation, but this has not been formally confirmed.

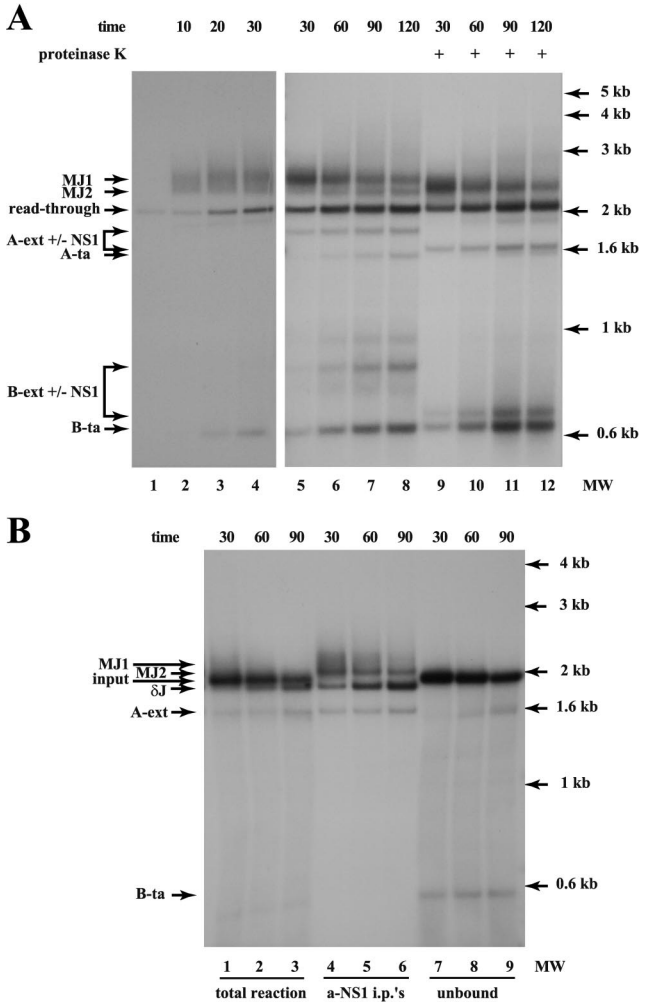

FIG. 4. Time course of resolution reactions. (A) Autoradiographs of 1.4% neutral agarose gels containing 0.2% SDS. Unlabeled templates, replicated in the presence of [α-^{32}P]TTP, are shown before (lanes 2 to 8) and after (lanes 9 to 12) digestion with proteinase K. For size comparison, ^{32}P-3′-labeled template is shown in lane 1. Samples were harvested after incubation for 10 min (lane 2), 20 min (lane 3), 30 min (lanes 4, 5, and 9), 60 min (lanes 6 and 10), 90 min (lanes 7 and 11), or 2 h (lanes 8 and 12). Fragments are labeled as detailed previously (Fig. 2B). (B) Autoradiograph of a 1.4% neutral agarose gel containing 0.2% SDS, showing the products of ^{32}P-3′-end-labeled substrates before (0.5× concentration, lanes 1 to 3) and after (lanes 4 to 6) immunoprecipitation with antiserum directed against NS1, or the unbound material from these precipitates (lane 7 to 9). Reaction products were harvested after incubation for 30 min (lanes 1, 4, and 7), 60 min (lanes 2, 5, and 8), or 90 min (lanes 3, 6, and 9).

New DNA associated with the more heterogeneous MJ1 intermediate migrated as an extended diagonal in the alkaline dimension, ranging from the position of an extended form of the B arm to the size of a B turn-around form in the more slowly migrating duplex MJ1 forms (Fig. 5A). Extrapolating from the MJ2 structure depicted in Fig. 5D, we suggest that MJ2 forms are likely converted to MJ1 forms by a hairpin transfer event that melts out the strands of the lower, extended-form, duplex and allows them to fold back on themselves, repositioning the 3′ nucleotide so that it primes synthesis back along the B arm. Accordingly, MJ1 forms would be heterogeneous, because they include a spectrum of molecules in which the returning fork has progressed to different lengths back along the B arm.

Two-dimensional analysis of 3′-end-labeled products (Fig. 5B) indicated that MJ1 and MJ2 intermediates were relatively minor species. Although the 3′-end-labeled forms associated with these intermediates were faint, they clearly contained one strand of ~1.6 kb, corresponding to a 3′-end-labeled form of the lower strand that had been nicked in the B arm at OriL_{TC}, and one full-length strand of 2.1 kb. This full-length strand is difficult to see for the MJ2 intermediate in Fig. 5B, since it migrates coincidentally with the residual input substrate; however, it can be readily detected in two-dimensional gels of 3′-labeled products immunoprecipitated by virtue of their covalent association with NS1, as shown at higher magnification in Fig. 5C, since residual input is not present in these precipitates. Thus, MJ2 (and MJ1) and products are in accord with those detailed in the proposed heterocruciform structure of the MJ2 intermediate as shown for 3′-end-labeled substrates in Fig. 5E, having one 3′-labeled intact strand and one 3′-labeled strand that has been nicked at OriL_{TC}, creating an extended form of the A arm.

Most notably, labeled forms of the B arm (0.5 to 1 kb) were not apparent in the 3′-end-labeled MJ intermediates shown in Fig. 5B, indicating that the B forms labeled so heavily by in vitro synthesis in Fig. 5A were most likely produced by nicking and extension of the lower strand of the B arm, which would not carry a 3′ end label, as illustrated in Fig. 5E.

Figures 5B and C also reveal the structure of the δJ intermediate. This structure was not visible in Fig. 5A because it contained no newly synthesized DNA, but in the products of the 3′-end-labeled substrates it could be seen to contain an intact 2.1-kb strand and a 1.6-kb extended-form A arm. Since it is also present in Fig. 5C it must carry a covalently associated NS1 molecule, but it migrates faster than substrate DNA in the neutral dimension, so that it must have lost some DNA, presumably the unlabeled lower strand of the B arm. We therefore suggest that δJ molecules (together with free turn-around forms of the B arm) are the products of MJ1 intermediates in which the returning fork has completed synthesis of the B turn-around structure, causing it to be released.

DISCUSSION

The products and intermediates of the in vitro dimer junction resolution reaction are complex, in part because two different types of reactions appear to be going on simultaneously. One of these, read-through synthesis, would provide an efficient mechanism for DNA amplification but would regenerate the duplex dimer intermediate rather than resolve the bridge structure into separate duplex telomeres. The second type of reaction, which provides the resolution pathway as described below, relies upon the ability of NS1 to induce the palindrome to undergo a duplex-to-hairpin transition, creating a resolution substrate in which the nick site in the A arm is ultimately exposed as a single strand.

In Fig. 6 we suggest a heterocruciform resolution model to explain how NS1 is able to bring about resolution of the dimer bridge into separate duplex telomeres while conserving the flip configuration of the hairpin on all negative-sense strands. This

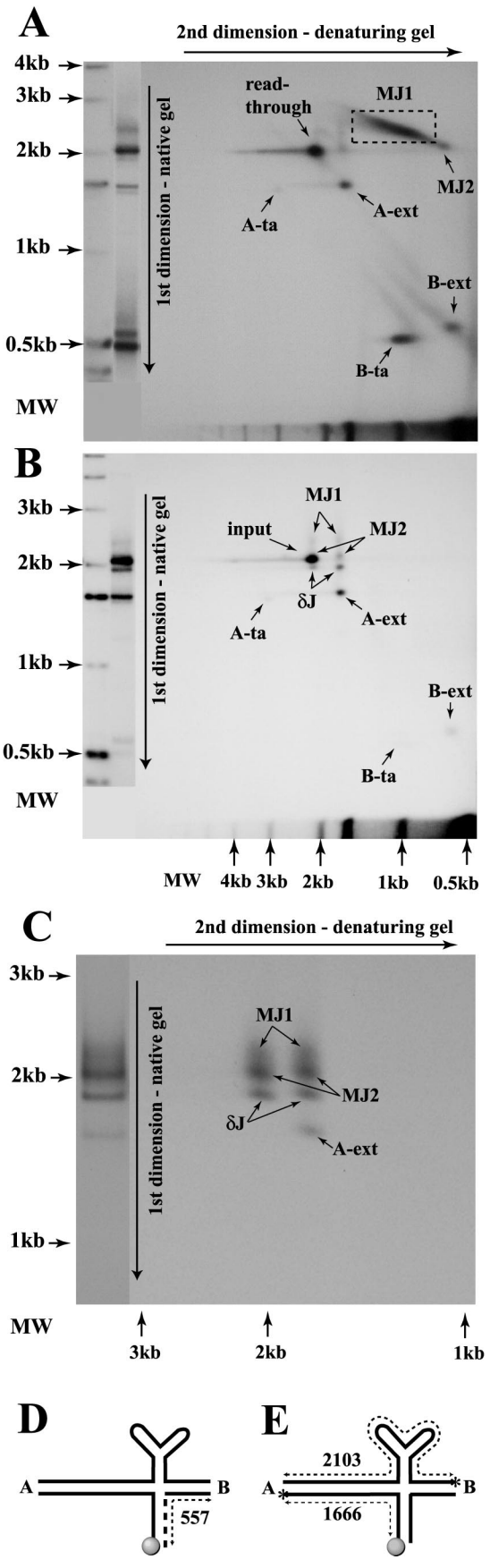

model takes into account the structures and apparent kinetic relationships between the various resolution intermediates and products observed above.

Read-through synthesis versus resolution. According to this model, NS1 initially introduces a site-specific, single-strand nick into $OriL_{TC}$, in the B arm of the bridge, becoming covalently attached to the DNA at the 5′ side of the nick and exposing a base-paired 3′ nucleotide (Fig. 6, step i). This reaction can be reproduced in vitro with 3′-labeled dimer bridge substrates in standard nicking assays using only recombinant NS1 and PIF (data not shown). NS1 would then be expected to bind RPA (9) and recruit it to the nick site, but two possible outcomes would ensue, depending upon the speed with which a replication fork was assembled on the exposed 3′ nucleotide. As illustrated in Fig. 3A, if a fork assembled rapidly while the bridge remained in the linear configuration, read-through synthesis would copy the upper strand, displacing a positive-sense single strand from the A arm and regenerating the duplex substrate. In vivo, in the context of an MVM infection, we would expect that the displaced positive-sense single strand would be converted rapidly into an extended-form duplex telomere by a fork arising from the origin at the right end of the viral genome. However, since our in vitro substrates lack right-end origins, the duplex resolution products we have observed must be generated by an alternative mechanism.

Formation of the cruciform resolution substrate. In order for resolution to occur, we suggest that the initial nicking event in $OriL_{TC}$ must be followed by melting and rearrangement of the bridge palindrome into a cruciform intermediate prior to fork assembly, allowing synthesis of new DNA in the flip orientation. Such duplex-to-hairpin rearrangements could be accomplished by a simple helicase mechanism, as illustrated in Fig. 6, steps ii to iv. In this pathway assembly of the fork is delayed, so that in the presence of RPA the NS1 3′-to-5′ helicase activity begins to unwind the duplex, as recently doc-

FIG. 5. Two-dimensional analysis of resolution products on native and denaturing gels. Samples were digested with proteinase K and subjected to electrophoresis under native conditions, as shown for a parallel track positioned along the left side of each panel. The sample lane was then subjected to electrophoresis, at 90° to the original direction, under alkaline, denaturing conditions. (A) Autoradiograph of a two-dimensional 1.4% agarose gel showing resolution products labeled by incorporation of [α-^{32}P]TTP into newly synthesized DNA, extracted after a 60-min reaction. Fragments are labeled as detailed in the legend for Fig. 2B. (B) Autoradiograph of a two-dimensional 1.4% agarose gel showing total resolution products of ^{32}P-3′-end-labeled templates, extracted after a 60-min reaction. Arrows indicate both of the 3′-labeled species originating from the single MJ1, MJ2, and δJ bands present in the neutral dimension. (C) Autoradiograph of a two-dimensional agarose gel showing resolution products of ^{32}P-3′-end-labeled templates, as in panel B but immunoprecipitated with anti-NS1 serum prior to proteinase K digestion. Regions containing the labeled resolution intermediates are enlarged relative to those shown in panels A and B, to allow discrimination of both the 2.1-kb and 1.6-kb spots derived from MJ1, MJ2, and δJ intermediates. (D) The probable configuration of MJ2 intermediates labeled by incorporation of [α-^{32}P]TTP into newly synthesized DNA (thick dahsed line). Dotted lines with arrows indicate the labeled fragment of 557 nucleotides. (E) The probable configuration of ^{32}P-3′-end-labeled MJ2 intermediates. Dotted lines with arrows indicate labeled fragments of 2,103 and 1,666 nucleotides.

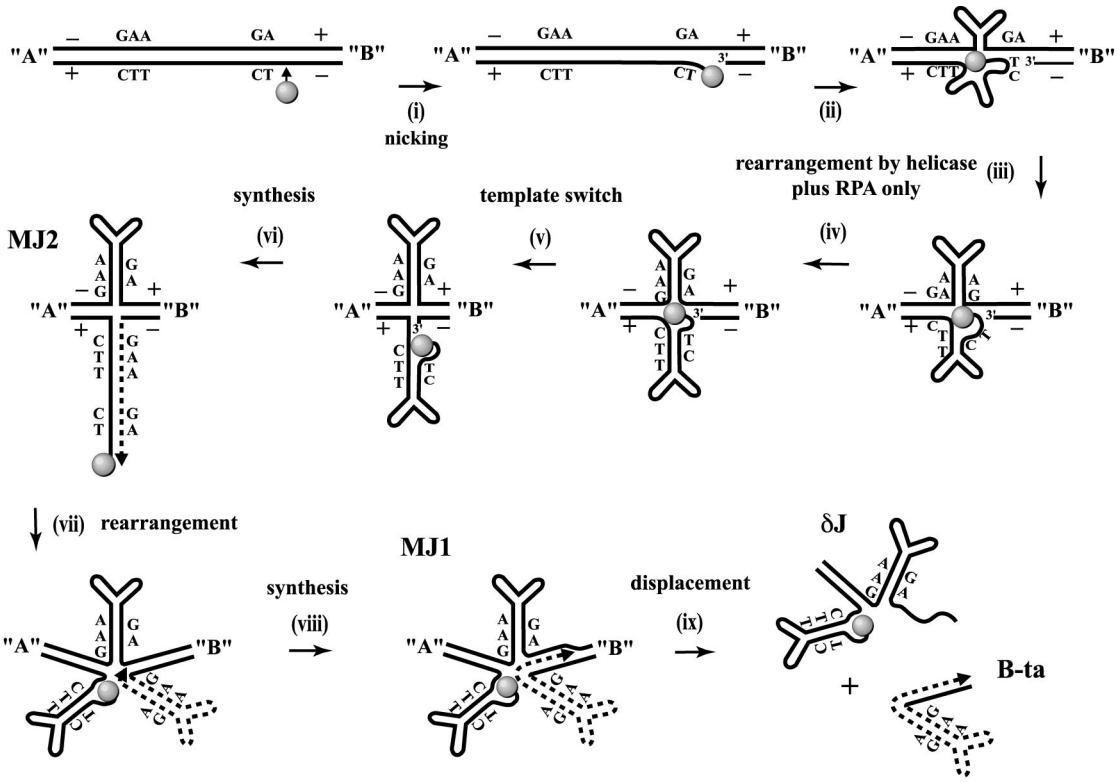

FIG. 6. The resolution pathway. After nicking the initiation site in the B arm of the dimer bridge (step i), NS1 associates with RPA to function as a 3′-to-5′ helicase (step ii), unwinding the lower strand of the palindrome and allowing the exposed single strands to fold back on themselves, creating a cruciform intermediate (step iii). Branch migration proceeds (step iv), eventually passing the inactive initiation site in the A arm. At this point the exposed 3′ nucleotide can switch templates and anneal to its complement in the lower cruciform arm (step v). A replication fork assembling at this time will copy and unwind the cruciform arm, synthesizing a palindrome in the flip orientation on the end of the negative-sense B strand (step vi). This heterocruciform structure corresponds to the MJ2 intermediate. In a second duplex-to-hairpin transition, the palindromic heterocruciform arm of MJ2 is then melted out and both strands fold back on themselves (step vii), allowing the exposed 3′ end to base-pair with inboard sequences in the B arm. A replication fork established at this 3′ end would copy the lower strand of the B arm (step viii), creating the MJ1 intermediate and progressively displacing the upper strand, leading to the eventual release of a newly synthesized B turn-around form (step ix). The residual δJ intermediate is partially single stranded, having an intact upper strand paired to an NS1-associated lower strand from the A arm. Since this complex carries the active helicase, it is presumed to be a dynamic structure in which the bridge palindrome is periodically reconfigured into a cruciform structure, as shown.

umented (9). As the helicase passes through the axis of symmetry, the two separated strands begin to fold back on themselves, and branch migration continues until the cruciform arms extend past the nick site (steps iii and iv).

Alternatively, NS1 may be able to melt out and reconfigure the MVM dimer bridge palindrome in an RPA-independent reaction. Willwand and colleagues (23) observed NS1-dependent, hairpin-primed replication at both termini of a duplex MVM DNA template using cell extracts in vitro, and they went on to show that purified NS1 was able to melt out extended forms of the MVM right-end telomere in the absence of cellular replication factors (22). This latter reaction was dependent upon the presence of both copies of the paired NS1 binding sites which surround the symmetry axis of the right-end telomere. Although plausible, at present there is no direct experimental evidence for comparable reactions involving extended-form left-end telomeres of MVM or the dimer bridge.

Synthesis of the heterocruciform. Once the cruciform extends to include sequences beyond the nick site in the A arm, the primer exposed at the nick site in $OriL_{TC}$ can undergo a template switch by annealing with its complement in the lower cruciform arm (Fig. 6, step v). If a replication fork assembles after this point, the resulting synthesis will unfold and copy the flop sequence of the lower cruciform arm, with NS1 perhaps again serving as the 3′-to-5′ helicase required for strand displacement. This would create a heterocruciform intermediate that contains a newly synthesized telomere in the flip orientation attached to the lower (−) strand of the B arm (step vi). Such a structure corresponds exactly to that of the MJ2 intermediate, as determined in Fig. 5.

We had previously suggested that a cellular or viral recombinase could resolve heterocruciform intermediates of this type, with directional specificity, into the expected termini (13, 14). However, such a reaction would transfer the labeled, newly synthesized DNA (depicted in step vi) onto an extended form of the A arm, leaving the B turn-around arm unlabeled. Since this is not compatible with our experimental data, in which turn-around forms of the B arm are seen to accumulate most of the newly synthesized DNA, we now conclude that a directional recombinase is not responsible for subsequent resolution.

Hairpin transfer and release of the B turn-around arm. We suggest that synthesis pauses after completion of the MJ2 intermediate because the fork reaches the end of its template strand (Fig. 6, step vi). Although evidence of a precursor-product relationship has not been established for the subsequent transition, we suggest that MJ2 forms are converted to MJ1 forms by a hairpin transfer event that allows the two strands of the lower heterocruciform arm to melt out and fold back on themselves, repositioning the exposed 3′ nucleotide on the B arm (Fig. 6, step vii) and allowing a new fork established on this primer to synthesize a B turn-around form (step viii). This hairpin transfer reaction could be mediated by either of the NS1-driven mechanisms discussed previously in relation to dimer bridge substrates. Thus, according to the new model, both creation of the heterocruciform and its subsequent resolution would be driven by the characteristic NS1-mediated duplex-to-hairpin rearrangements of the palindrome that are the hallmark of parvovirus DNA amplification.

Upon completion of the B turn-around structure, it would be released from the MJ1 intermediate (Fig. 6, step ix), leaving a δJ intermediate which consists of one intact DNA strand base-paired to an extended form of the A arm. Since the A arm of this intermediate has an NS1-associated, recessed 5′ end, the 3′-to-5′ helicase activity of NS1 would again tend to unwind the lower strand of the palindrome, allowing the single strands to fold back on themselves and creating the branched intermediate depicted in Fig. 6.

Introduction of a single-strand nick and resolution of the δJ intermediate. In the absence of a large excess of RPA, the helicase activity of NS1 rarely manages to fully displace the lower strand of the δJ intermediate (Fig. 3B), but it likely creates a dynamic structure in which the nick site in the inactive A arm ($OriL_{GAA}$) is transiently, but repeatedly, exposed in a single-stranded form. We speculate that under these conditions $OriL_{GAA}$ can be nicked by free NS1 in a PIF-independent reaction (Fig. 7, steps i and ii). This type of single-stranded nicking reaction could also occur on MJ1 and MJ2 intermediates, perhaps bypassing release of the δJ form. However, δJ forms do accumulate, suggesting that the postulated single-strand nicking reaction may be inefficient or that NS1 becomes limiting at late times in vitro.

This final nick would leave NS1 covalently attached to a positive-sense B arm (Fig. 7, step ii), which would be released from the complex by strand displacement synthesis from the new 3′ nucleotide exposed at the nick site, generating a new extended form of the A arm (Fig. 7, step iv). In vivo, in the context of the MVM genome, this single-strand nick may be a rare event. This is because both ends of dimer RF bear efficient "right-end" hairpin origins and, in vivo, forks may proceed back towards the dimer bridge from the right end of the genome, along the top strand of the B arm, at the same time that a turn-around form of the B arm is being released from MJ1-like intermediates. This would effectively bypass dimer bridge resolution, recycling the top strand into a replicating duplex dimer pool. Since we show here that there is a mechanism which will allow NS1 to bring about the full resolution of dimer bridge structures into duplex forms of the two arms, we suggest that, in vivo, which process dominates may depend, to a surprising extent, upon the efficiency of the origins at the right end of the genome.

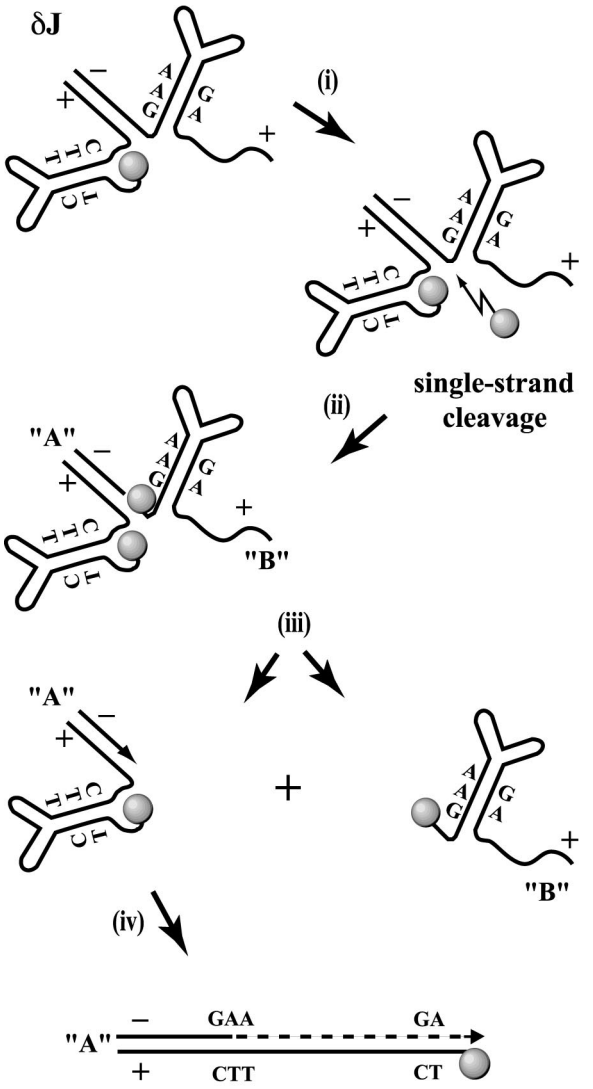

FIG. 7. Introduction of a single-strand nick and resolution of the δJ intermediate. The initiation site in the A arm of the palindrome is periodically exposed as a single strand during duplex-to-hairpin rearrangements of δJ (step i). This allows NS1 to attack the initiation site in $OriL_{GAA}$ without the help of a cofactor (step ii). Nicking leads to the release of a positive-sense B strand and leaves a base-paired 3′ nucleotide on the A arm (step iii) to prime assembly of a fork which will copy the hairpin, creating an extended form of the A arm (step iv).

Although all other termini generated in this resolution pathway are in the flip orientation, the final single-stranded nick would generate a positive-sense strand with a flop hairpin in which the three-nucleotide bubble sequence, GAA, is positioned in the outer arm. Although such telomeres were not observed in vivo for MVM (1), they have been identified in the closely related virus LuIII (5). Unlike MVM, LuIII packages DNA strands of both senses with equal efficiency (4), and while the left-end hairpins of its negative-sense strands are all in the flip orientation, in positive-sense strands flip and flop orientations are expressed with equal frequency (5). We suggest that there could be two different mechanisms for processing δJ intermediates and that the balance between these that is

achieved in vivo is determined by the rate of hairpin transfer at the right end of the viral genome. Since the orientation of termini excised by these two mechanisms is somewhat different, one way to test this prediction experimentally would be to impair the efficiency of the MVM right-end origin by genetic manipulation.

Preliminary experiments indicate that nature has already explored this avenue. We are currently mapping the sequences in the LuIII genome which allow it to package all of the resolution products predicted from the heterocruciform model, and we find that this ability maps to a 2-nucleotide insertion in the NS1 nick site of the right-end origin. This insertion has the effect of making the LuIII origin refractory to nicking when compared in vitro to its MVM counterpart. Thus, when the right-end hairpin of LuIII is substituted for the equivalent MVM sequence, a virus is generated which has a slow right-end origin and which packages, in addition to negative-sense strands, positive strands whose left-end termini exist in both flip and flop orientations (S. F. Cotmore and P. Tattersall, unpublished data).

This observation suggests that any genome-length single strand which is excised from replicative-form concatemers will ultimately be packaged, and that it is only the failure to excise certain termini efficiently which precludes their encapsidation. Hence, it predicts that there are no specific sequences in MVM or LuIII DNA that allow the selection of negative- versus positive-sense strands for packaging. In this respect the heterocruciform model potentially provides a mechanistic perspective from which to view the earlier kinetic hairpin transfer model of parvovirus DNA replication (5). This mathematical model was based purely on physical measurements of terminal sequence heterogeneity and the ratio of plus to minus strands packaged into virions by different parvoviruses, and it suggested that all such heterogeneity could be explained simply by the relative rates of hairpin transfer at the right and left ends of each genome. Although this model had many interesting implications, it was difficult to reconcile with our knowledge of viral biochemistry, since we have long been aware that left-end termini of viruses such as MVM and LuIII are excised by resolution of the dimer intermediate and not simply by hairpin transfer reactions. The data presented in this paper may therefore provide a conceptual basis for reconciling the earlier mathematical model with specific biochemical mechanisms.

ACKNOWLEDGMENT

This work was supported by U.S. Public Health Service grant number AI26109 from the National Institute of Allergy and Infectious Diseases.

REFERENCES

1. **Astell, C. R., M. B. Chow, and D. C. Ward.** 1985. Sequence analysis of the termini of virion and replicative forms of minute virus of mice DNA suggests a modified rolling hairpin model for autonomous parvovirus DNA replication. J. Virol. **54:**171–177.
2. **Astell, C. R., M. Thomson, M. B. Chow, and D. C. Ward.** 1983. Structure and replication of minute virus of mice DNA. Cold Spring Harbor Symp. Quant. Biol. **47:**751–762.
3. **Baldauf, A. Q., K. Willwand, E. Mumtsidu, J. P. Nuesch, and J. Rommelaere.** 1997. Specific initiation of replication at the right-end telomere of the closed species of minute virus of mice replicative-form DNA. J. Virol. **71:**971–980.
4. **Bates, R. C., C. E. Snyder, P. T. Banerjee, and S. Mitra.** 1984. Autonomous parvovirus LuIII encapsidates equal amounts of plus and minus DNA strands. J. Virol. **49:**319–324.
5. **Chen, K. C., J. J. Tyson, M. Lederman, E. R. Stout, and R. C. Bates.** 1989. A kinetic hairpin transfer model for parvoviral DNA replication. J. Mol. Biol. **208:**283–296.
6. **Christensen, J., S. F. Cotmore, and P. Tattersall.** 2001. Minute virus of mice initiator protein NS1 and a host KDWK family transcription factor must form a precise ternary complex with origin DNA for nicking to occur. J. Virol. **75:**7009–7017.
7. **Christensen, J., S. F. Cotmore, and P. Tattersall.** 1997. A novel cellular site-specific DNA-binding protein cooperates with the viral NS1 polypeptide to initiate parvoviral DNA replication. J. Virol. **71:**1405–1416.
8. **Christensen, J., S. F. Cotmore, and P. Tattersall.** 1999. Two new members of the emerging KDWK family of combinatorial transcription modulators bind as a heterodimer to flexibly spaced PuCGPy half-sites. Mol. Cell. Biol. **19:**7741–7750.
9. **Christensen, J., and P. Tattersall.** 2002. Parvovirus initiator protein NS1 and RPA coordinate replication fork progression in a reconstituted DNA replication system. J. Virol. **76:**6518–6531.
10. **Cotmore, S. F., J. P. Nuesch, and P. Tattersall.** 1993. Asymmetric resolution of a parvovirus palindrome in vitro. J. Virol. **67:**1579–1589.
11. **Cotmore, S. F., J. P. Nuesch, and P. Tattersall.** 1992. In vitro excision and replication of 5′ telomeres of minute virus of mice DNA from cloned palindromic concatemer junctions. Virology **190:**365–377.
12. **Cotmore, S. F., and P. Tattersall.** 1994. An asymmetric nucleotide in the parvoviral 3′ hairpin directs segregation of a single active origin of DNA replication. EMBO J. **13:**4145–4152.
13. **Cotmore, S. F., and P. Tattersall.** 1996. Parvovirus DNA replication, p. 799–813. *In* M. DePamphilis (ed.), DNA replication in eukaryotic cells. Cold Spring Harbor Laboratory Press, Cold Spring Harbor, N.Y.
14. **Cotmore, S. F., and P. Tattersall.** 1995. DNA replication in the autonomous parvoviruses. Semin. Virol. **6:**271–281.
15. **Cotmore, S. F., and P. Tattersall.** 1998. High-mobility group 1/2 proteins are essential for initiating rolling-circle-type DNA replication at a parvovirus hairpin origin. J. Virol. **72:**8477–8484.
16. **Cotmore, S. F., and P. Tattersall.** 1992. In vivo resolution of circular plasmids containing concatemer junction fragments from minute virus of mice DNA and their subsequent replication as linear molecules. J. Virol. **66:**420–431.
17. **Liu, Q., C. B. Yong, and C. R. Astell.** 1994. In vitro resolution of the dimer bridge of the minute virus of mice (MVM) genome supports the modified rolling hairpin model for MVM replication. Virology **201:**251–262.
18. **Muzyczka, N., and K. I. Berns.** 2001. Parvoviridae: the viruses and their replication, p. 2327–2360. *In* D. M. Knipe and P. M. Howley (ed.), Fields virology, 4th ed. Lippincott Williams and Wilkins, Philadelphia, Pa.
19. **Nuesch, J. P., J. Christensen, and J. Rommelaere.** 2001. Initiation of minute virus of mice DNA replication is regulated at the level of origin unwinding by atypical protein kinase C phosphorylation of NS1. J. Virol. **75:**5730–5739.
20. **Nuesch, J. P., R. Corbau, P. Tattersall, and J. Rommelaere.** 1998. Biochemical activities of minute virus of mice nonstructural protein NS1 are modulated in vitro by the phosphorylation state of the polypeptide. J. Virol. **72:**8002–8012.
21. **Tattersall, P., and D. C. Ward.** 1976. Rolling hairpin model for replication of parvovirus and linear chromosomal DNA. Nature (London) **263:**106–109.
22. **Willwand, K., A. Moroianu, R. Horlein, W. Stremmel, and J. Rommelaere.** 2002. Specific interaction of the nonstructural protein NS1 of minute virus of mice (MVM) with [ACCA](2) motifs in the centre of the right-end MVM DNA palindrome induces hairpin-primed viral DNA replication. J. Gen. Virol. **83:**1659–1664.
23. **Willwand, K., E. Mumtsidu, G. Kuntz-Simon, and J. Rommelaere.** 1998. Initiation of DNA replication at palindromic telomeres is mediated by a duplex-to-hairpin transition induced by the minute virus of mice nonstructural protein NS1. J. Biol. Chem. **273:**1165–1174.
24. **Wobbe, C. R., F. Dean, L. Weissbach, and J. Hurwitz.** 1985. In vitro replication of duplex circular DNA containing the simian virus 40 DNA origin site. Proc. Natl. Acad. Sci. USA **82:**5710–5714.